

Structural and magnetic properties of the layered manganese oxychalcogenides $(\text{LaO})_2\text{Mn}_2\text{Se}_2\text{O}$ and $(\text{BaF})_2\text{Mn}_2\text{Se}_2\text{O}$

R. H. Liu, J. S. Zhang, P. Cheng, X. G. Luo, J. J. Ying, Y. J.

Yan, M. Zhang, A. F. Wang, Z. J. Xiang, G. J. Ye and X. H. Chen*

*Hefei National Laboratory for Physical Science at Microscale and Department of Physics,
University of Science and Technology of China, Hefei, Anhui 230026, People's Republic of China*

The new layered manganese oxychalcogenides $(\text{LaO})_2\text{Mn}_2\text{Se}_2\text{O}$ and $(\text{BaF})_2\text{Mn}_2\text{Se}_2\text{O}$, isostructural to $(\text{LaO})_2\text{Fe}_2\text{Se}_2\text{O}$, were synthesized by using solid state reaction. The single crystals of the former compound were also successfully grown using fusion method. The polycrystalline samples show the semiconducting behavior with the activation energy gaps of about 278 meV and 416 meV for $(\text{LaO})_2\text{Mn}_2\text{Se}_2\text{O}$ and $(\text{BaF})_2\text{Mn}_2\text{Se}_2\text{O}$, respectively. The magnetic susceptibility and specific heat indicate an antiferromagnetic (AFM) transition at around 160 ± 1 K for the former compound and 100 ± 1 K for the second compound. The strong anisotropic magnetic properties below T_N of the former compound suggests a long-range canted AFM ordering. A broad maximum of the susceptibility can be observed for the two compounds at high temperatures of 360 K and 210 K, respectively, suggesting that strong frustrated magnetic correlation gives rise to low-dimensional AFM or short-range ordering at high temperatures in these rare transition metal oxychalcogenides with an AFM checkerboard spin lattice.

PACS numbers: 81.05±t, 75.30±m, 75.40±s, 71.27.+a

I. INTRODUCTION

Low-dimensional spin systems have received considerable attention because of the possible emergence of novel physics such as superconductivity[1–4], colossal magnetoresistance (CMR)[5], giant thermoelectric power (GTP)[6] etc. The parent compound of high- T_c cuprates is antiferromagnetic (AFM) Mott insulator with a square lattice of copper[7]. The recently discovered iron-based pnictides are the spin-density-wave type (SDW-type) AFM bad metal[8–10]. They are also placed at the boundary of itinerancy and Mott localization in many studies[11, 12]. Furthermore, the CMR materials also evolve from Mott insulators by doping[13]. It is very important to understand the correlated electron structure and magnetic properties of those Mott insulators, which helps people to study the novel physics. The discovery of non-copper high- T_c iron-based pnictides with two-dimensional FeAs layers received intense interests in the layered transition-metal oxychalcogenides[14] or oxypnictides[15]. These compounds share a common square lattice of the transition-metal. The titanium oxypnictides RTi_2Pn_2O ($R = \text{Na}_2, \text{Ba}, (\text{SrF})_2$ and $(\text{SmO})_2$, $Pn = \text{As}$ and Sb)[14, 16–22] have a SDW/charge-density-wave (CDW) instability corresponding to an anomalous transition in resistivity, susceptibility and Hall coefficient etc, similar to the properties of iron pnictides. The transition metal oxychalcogenides $R_2\text{Fe}_2Q_2\text{O}$ ($R = (\text{BaF}), (\text{SrF})$ and (LaO) , $Q = \text{S}$ and Se)[15, 23] are isostructural to the titanium oxypnictides. The previous studies found that the Fe analogues formed a long-range AFM ordering below $83\text{ K}\sim 106\text{ K}$

and were Mott insulators due to the narrowing of the Fe d -electron bands and corresponding enhancement of correlation effects[24]. More recently, Wang et al[25] synthesized $(\text{LaO})_2\text{Co}_2\text{Se}_2\text{O}$, and found that it was insulator and had an AFM transition at $T_N \sim 220\text{ K}$. Moreover, the authors suggested that the Co analogues had an unusual low-spin (LS, $S=1/2$) state of the Co^{2+} ions and a corresponding orbital polarization. However, Wu et al[26] suggested that the square-lattice Mott insulator $\text{La}_2\text{O}_2\text{Co}_2\text{Se}_2\text{O}$ had more stable high-spin (HS, $S=3/2$) ground state with a considerably strong magnetic frustration.

In the present work, we synthesize other new manganese oxychalcogenides $R_2\text{Mn}_2\text{Se}_2\text{O}$ ($R = (\text{LaO})$ and (BaF)), which are isostructural to the previous Fe and Co analogues. In addition, we perform the anisotropic measurements of magnetic susceptibility in single crystal $\text{La}_2\text{O}_2\text{Mn}_2\text{Se}_2\text{O}$. These intrinsic behaviors are helpful in understanding the underlying magnetism of the transition-metal oxychalcogenides.

II. EXPERIMENTAL DETAILS

Polycrystalline samples of $(\text{LaO})_2\text{Mn}_2\text{Se}_2\text{O}$ and $(\text{BaF})_2\text{Mn}_2\text{Se}_2\text{O}$ were synthesized by solid state reaction method using BaF_2 (3N), BaO (3N), La_2O_3 (3N), MnSe powder as starting materials. MnSe was pre-synthesized by heating the mixture of Se (3N) powder and Mn (3N) powder in an evacuated quartz tube from room temperature to $750\text{ }^\circ\text{C}$ in 12 hours and staying at $750\text{ }^\circ\text{C}$ for 24 hours. La_2O_3 was dried by heating in air at $900\text{ }^\circ\text{C}$ for 20 hours before using. The raw materials and precursors were weighed according to the stoichiometric ratio of $(\text{BaF})_2\text{Mn}_2\text{Se}_2\text{O}$ or $(\text{LaO})_2\text{Mn}_2\text{Se}_2\text{O}$, thoroughly grounded, pressed into pellets and then sealed in evacu-

*Corresponding author; Electronic address: chenxh@ustc.edu.cn

ated quartz tubes. The sealed tubes were sintered at 1000 °C for 40 hours for $(\text{LaO})_2\text{Mn}_2\text{Se}_2\text{O}$ samples and 800 °C for 60 hours for $(\text{BaF})_2\text{Mn}_2\text{Se}_2\text{O}$ samples. In order to improve their purity and homogeneity, the resulting products were reground in argon atmosphere before applying a second heat treatment at the same temperature. To grow single crystal, the formed $(\text{LaO})_2\text{Mn}_2\text{Se}_2\text{O}$ pellets were loaded into an alumina crucible and then sealed in evacuated quartz tube. The tube was slowly heated to 1300 °C at a rate of 5 °C/min and kept at 1300 °C for 10 hours. Subsequently, the temperature was lowered slowly to 1000 °C in 40 hours, and then the quartz tube was cooled in the furnace by shutting off the power. The black single crystals can be yielded at the bottom of the alumina crucible. The sample preparation processes except for heating were carried out in the glove box with highly pure argon atmosphere filled.

X-ray powder diffraction and single crystal diffraction were both carried out on TTRAX3 theta/theta rotating anode X-ray Diffractometer (Japan) with Cu $K\alpha$ radiation and a fixed graphite monochromator. The powder diffraction data was collected in the $5 \sim 115^\circ 2\theta$ range at room temperature. The lattice parameters and the crystal structures were refined by using the Rietveld method in the programs GSAS package, applying Thompson-Cox-Hastings functions with asymmetry corrections as reflection profiles. Direct current (DC) magnetic susceptibility measurement was performed by using a SQUID magnetometer (Quantum Design MPMS-XL7s). The dc electrical resistivity was measured on the Quantum Design PPMS with four probes for $(\text{LaO})_2\text{Mn}_2\text{Se}_2\text{O}$ and two probes for $(\text{BaF})_2\text{Mn}_2\text{Se}_2\text{O}$.

III. RESULTS AND DISCUSSION

TABLE I: Atomic coordinates and equivalent isotropic displacement parameters (U_{iso}) for $R_2\text{Mn}_2\text{Se}_2\text{O}$ ($R = (\text{LaO})$ and (BaF)).

atom	site	x	y	z	$U_{iso}(\text{\AA}^2)$
$(\text{LaO})_2\text{Mn}_2\text{Se}_2\text{O}$					
La	4e	1/2	1/2	0.18626(4)	0.0017(3)
O	4d	1/2	0	1/4	0.004(2)
Mn	4c	1/2	0	0	0.0121(7)
Se	4e	0	0	0.09984(7)	0.0076(4)
O	2a	1/2	1/2	0	0.033(5)
$(\text{BaF})_2\text{Mn}_2\text{Se}_2\text{O}$					
Ba	4e	1/2	1/2	0.17207(5)	0.0209(1)
F	4d	1/2	0	1/4	0.0437(2)
Mn	4c	1/2	0	0	0.0246(5)
Se	4e	0	0	0.09445(4)	0.0277(2)
O	2a	1/2	1/2	0	0.0148(4)

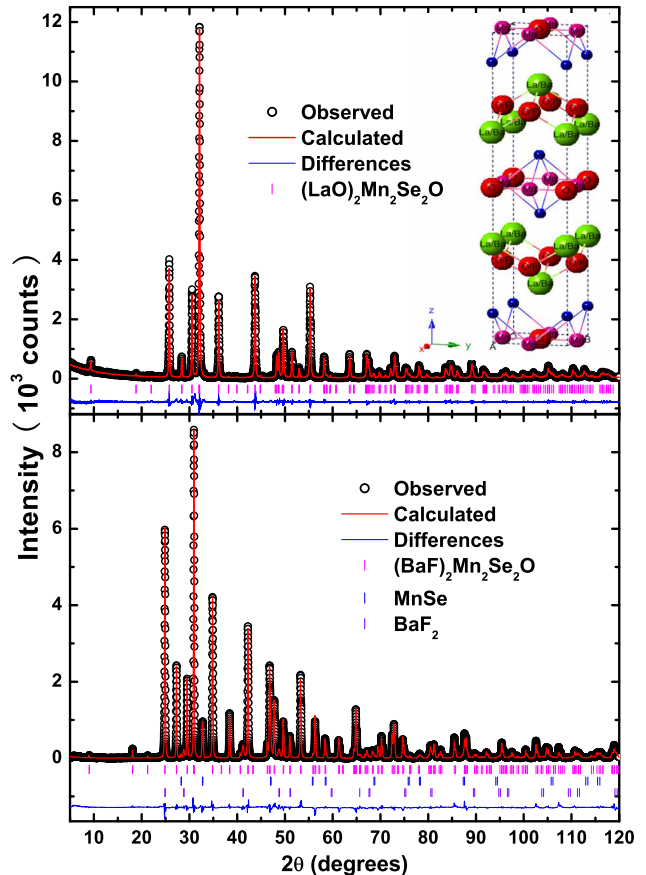


FIG. 1: X-ray powder diffraction patterns at room temperature for $(\text{LaO})_2\text{Mn}_2\text{Se}_2\text{O}$ (top panel), and $(\text{BaF})_2\text{Mn}_2\text{Se}_2\text{O}$ (bottom panel). The solid line indicates the intensities calculated using the Rietveld method. The bottom solid curves show the differences between the observed and calculated intensities. The vertical short lines indicate the Bragg peak positions of the target compounds, respectively. Inset of top panel: Crystal structure of $R_2\text{Mn}_2\text{Se}_2\text{O}$ ($R = (\text{LaO})$ and (BaF)).

A. Structure Refinements

Figure 1 shows X-ray powder diffraction patterns for the samples $R_2\text{Mn}_2\text{Se}_2\text{O}$ ($R = (\text{LaO})$ (top panel) and (BaF) (bottom panel)). All the XRD reflections for the former compound, $(\text{LaO})_2\text{Mn}_2\text{Se}_2\text{O}$, can be indexed with a tetragonal unit cell. The data were well fitted by using the structure model of $(\text{LaO})_2\text{Fe}_2\text{Se}_2\text{O}$ with the space group of $I4/mmm$. As shown in inset of Fig.1, those Mn-based compounds are isostructural with Fe and Co oxychalcogenides and Ti oxypnictides. These layered compounds are stacked alternately with the fluorite type $[\text{Ln}_2\text{O}_2]$ or $[\text{AE}_2\text{F}_2]$ (Ln = rare earth metals, and AE =alkali earth metals) and edge-shared $M_2Pn_2\text{O}$ layers (M = transition metal, Pn = chalcogenide and pnictide). In the $M_2Pn_2\text{O}$ unit, $M_2\text{O}$ forms a square planar with anticonfiguration to the CuO_2 layer of high-

TABLE II: Cell parameters , selected interatomic distances, bond angles and reliability factors obtained using Rietveld refinements of $R_2\text{Mn}_2\text{Se}_2\text{O}$ ($R = (\text{LaO})$ and (BaF)) (Space group I4/mmm).

	$(\text{LaO})_2\text{Mn}_2\text{Se}_2\text{O}$	$(\text{BaF})_2\text{Mn}_2\text{Se}_2\text{O}$
Space group	I4/mmm	I4/mmm
a(Å)	4.14097(7)	4.2756(1)
c(Å)	18.8588(4)	19.5919(4)
V(Å ³)	323.38(2)	358.73(2)
Z	2	2
Data points	11500	11500
R _{wp} (%)	0.1067	0.1150
R _p (%)	0.0751	0.1066
Bond lengths(Å)		
d _{La-O} or d _{Ba-F}	2.3941(4)×4	2.62701(3)×4
d _{La-Se} or d _{Ba-Se}	3.3511(7)×4	3.38429(4)×4
d _{Mn-O}	2.07049(4)×2	2.13784(3) ×2
d _{Mn-Se}	2.7986(9)×4	2.82752(3)×4
d _{Mn-Mn}	2.92811(5)×4	3.02336(5)×4
Bond angles(°)		
O-La-O or F-Ba-F	75.399(1)×4	70.261(1)×4
	119.724(1)×4	108.936(1)×4
Mn-Se-Mn	63.086(1)×4	64.639(1)×4
	95.434(1)×4	98.242(1)×4

T_c cuprates, while two Pn are located above and below the center of this square unit. For such Se/O mixed tetragonal structure, according to Goodenough-Kanamori rules[27, 28], there are three intralayer spin exchange interactions: AF exchange J_1 via corner sharing Mn-O-Mn, AF exchange J_2 via face sharing Mn-O-Mn/Mn-Se-Mn and FM exchange J_3 via edge sharing Mn-Se-Mn. These spin exchange interactions induce magnetic frustration in these compounds with checkerboard spin lattice. According to our Rietveld refinement, we also know that, for $(\text{BaF})_2\text{Mn}_2\text{Se}_2\text{O}$, there are little impurity phases of BaF₂ and MnSe in XRD patterns. The data were well fitted by the targeted tetragonal phase and these impurity phases in structure refinement. The refined lattice parameters ($a = 4.14097(7)\text{Å}$ and $c = 18.8588(4)\text{Å}$ for $(\text{LaO})_2\text{Mn}_2\text{Se}_2\text{O}$; $a = 4.2756(1)\text{Å}$ and $c = 19.5919(4)\text{Å}$ for $(\text{BaF})_2\text{Mn}_2\text{Se}_2\text{O}$) are larger than those of the Fe and Co analogues due to Mn²⁺ ions being relatively larger than Fe²⁺ and Co²⁺ ions. The interatomic distance of Mn-Mn (2.928 Å) is smaller than that of rock salt structure MnO (3.142 Å) with an T_N~118 K antiferromagnetic order[29]. The detailed results of the Rietveld refinements are listed in Tables 1 and 2.

To get more information by comparing with other analogues, we measured temperature dependence of resistivity for the as-prepared $(\text{LaO})_2\text{Mn}_2\text{Se}_2\text{O}$ and $(\text{BaF})_2\text{Mn}_2\text{Se}_2\text{O}$ samples and found that they both show semiconducting behavior. The room tempera-

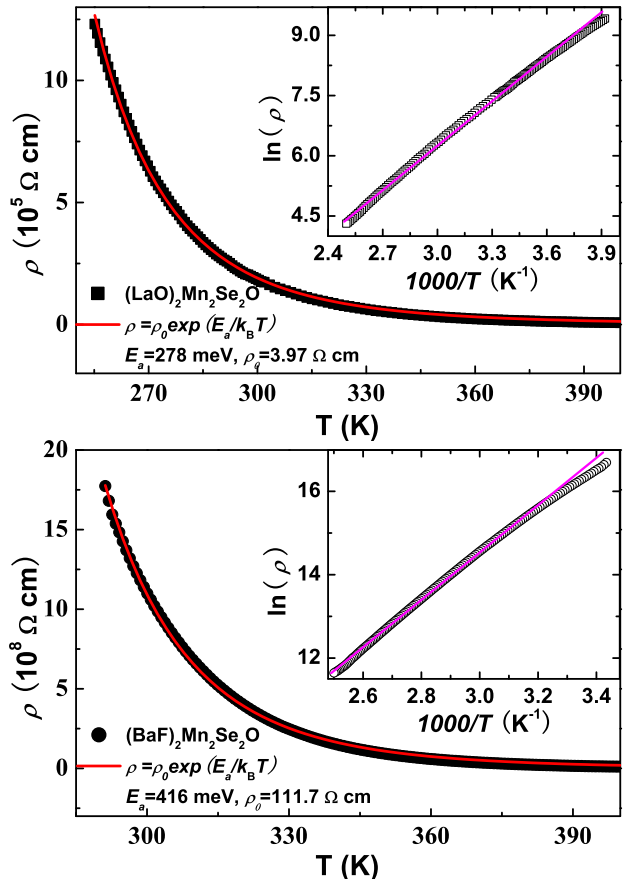


FIG. 2: Temperature dependence of resistivity ρ for polycrystalline $(\text{LaO})_2\text{Mn}_2\text{Se}_2\text{O}$ (top panel) and $(\text{BaF})_2\text{Mn}_2\text{Se}_2\text{O}$ (bottom panel). The solid line indicates the curves fitted using the Arrhenius equation $\rho = \rho_0 \exp(E_a/k_B T)$. Insets: The natural logarithm of resistivity $\ln \rho$ plotted against reciprocal of temperature.

ture resistivity is as high as $\sim 10^5$ and $10^9 \Omega \text{ cm}$, respectively, being three or six orders of magnitude higher than those of $(\text{LaO})_2\text{Fe}_2\text{Se}_2\text{O}$ ($10^2 \Omega \text{ cm}$) and $(\text{BaF})_2\text{Fe}_2\text{Se}_2\text{O}$ ($10^3 \Omega \text{ cm}$). In addition, the resistivity obeys thermally activated behavior (as shown in inset of Fig.2), and can be fitted by the Arrhenius equation: $\rho = \rho_0 \exp(E_a/k_B T)$, where ρ_0 is the pre-exponential factor and k_B is the Boltzmann constant. The obtained activation energy E_a is 278 meV for $(\text{LaO})_2\text{Mn}_2\text{Se}_2\text{O}$, which is located between Fe analogue (190 meV) and Co analogue (350 meV). The previous studies indicated that the Fe and Co analogues were Mott insulators with narrowing 3d electronic bands due to strong correlation effects. Our results may suggest that the Mn oxychalcogenides are also correlation-induced insulators with low-energy spin excitations (AFM) at low temperatures. For $(\text{BaF})_2\text{Mn}_2\text{Se}_2\text{O}$, there is larger activation energy (416 meV) with higher resistivity. It can be explained from the viewpoint of electron-hopping between adjacent spin sites. From the Rietveld refinement results above, one

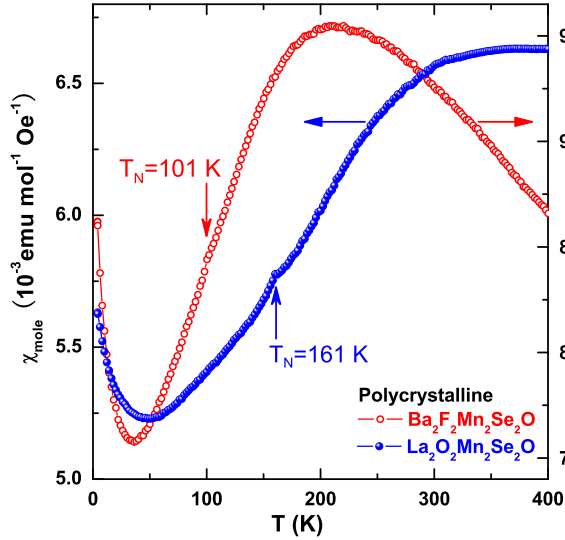


FIG. 3: Temperature dependence of magnetic susceptibility measured under $H=5$ T for polycrystalline samples of $R_2\text{Mn}_2\text{Se}_2\text{O}$ ($R = (\text{LaO})$ and (BaF)).

can easily see that the $(\text{LaO})_2\text{Mn}_2\text{Se}_2\text{O}$ has a greater integral for hopping between adjacent Mn^{2+} sites because it has shorter Mn...Mn, Mn-Se-Mn and Mn-O-Mn distances than those of $(\text{BaF})_2\text{Mn}_2\text{Se}_2\text{O}$.

Figure 3 shows the temperature dependence of the DC magnetic susceptibility $\chi(T)$ obtained at 5 T for $(\text{LaO})_2\text{Mn}_2\text{Se}_2\text{O}$ and $(\text{BaF})_2\text{Mn}_2\text{Se}_2\text{O}$ polycrystalline samples with the temperature ranging from 4 K to 400 K. The $\chi(T)$ of polycrystalline $(\text{LaO})_2\text{Mn}_2\text{Se}_2\text{O}$ shows a broad maximum around 360 K, suggesting the existence of a low-dimensional antiferromagnetism or a two-dimensional short-range ordering. Below 360 K, $\chi(T)$ decreases with reducing temperature to 50 K. In this decreasing $\chi(T)$, a small anomaly is observed at 161 K, which may suggest a magnetic transition occurring at this temperature. A broad maximum can also be observed in the $\chi(T)$ for polycrystalline $(\text{BaF})_2\text{Mn}_2\text{Se}_2\text{O}$ sample, at a temperature of 210 K. The different temperature corresponding to the maximum $\chi(T)$ for the two compounds indicate that $(\text{LaO})_2\text{Mn}_2\text{Se}_2\text{O}$ has a stronger AF coupling than $(\text{BaF})_2\text{Mn}_2\text{Se}_2\text{O}$ does. Combining with structural parameters listed in Table 2, it suggests that the chemical pressure effect enhances the spin exchange interactions. A similar behavior has been observed in isostructural Fe analogues[23]. A very slight anomaly also is observed around 101 K for $\chi(T)$ of $(\text{BaF})_2\text{Mn}_2\text{Se}_2\text{O}$. However, the obvious Curie paramagnetic tail at low temperature may arise from the small amount of impurity phase.

To shed light on the nature of the anomaly at 161 K in $\chi(T)$ of $(\text{LaO})_2\text{Mn}_2\text{Se}_2\text{O}$, we measured the DC magnetic susceptibility on the single crystal $(\text{LaO})_2\text{Mn}_2\text{Se}_2\text{O}$ sample with the magnetic field applied in ab -plane and along

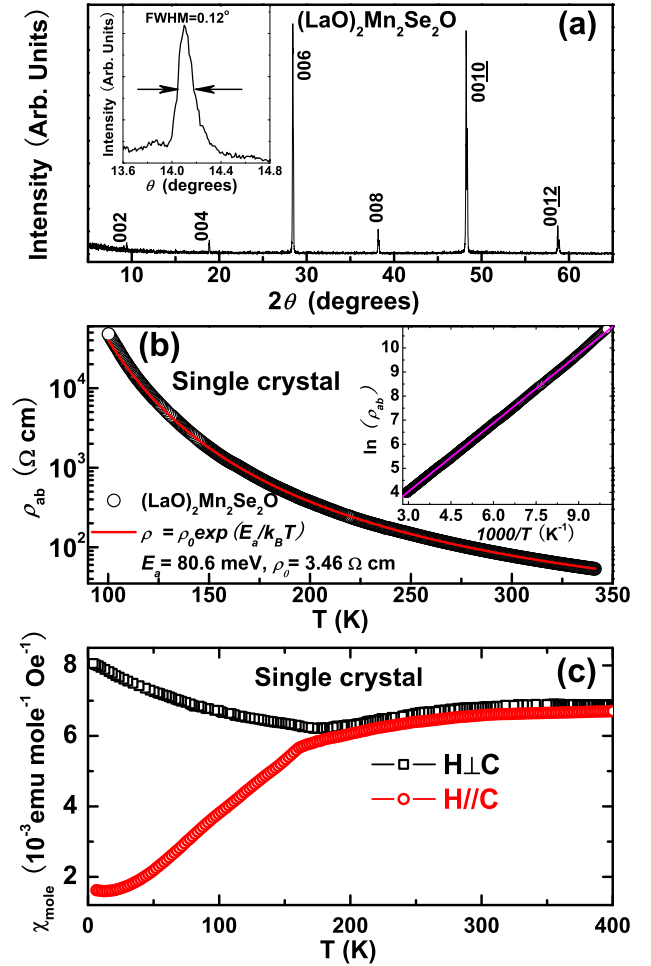


FIG. 4: (a) Single crystal x-ray diffraction pattern of $(\text{LaO})_2\text{Mn}_2\text{Se}_2\text{O}$. Only $(00l)$ diffraction peaks show up, suggesting that the c axis is perpendicular to the plane of the plate; Inset of top panel: rocking curve of (006) reflection. (b) Temperature dependence of resistivity ρ_{ab} for single crystal $(\text{LaO})_2\text{Mn}_2\text{Se}_2\text{O}$. Inset: The natural logarithm of resistivity $\ln \rho$ plotted against reciprocal of temperature. (c) Temperature dependence of magnetic susceptibility measured under $H=7$ T applied along the ab -plane (black), along the c -axis (red) of $(\text{LaO})_2\text{Mn}_2\text{Se}_2\text{O}$ single crystal, respectively.

c -axis. From the XRD patterns in Fig. 4a, only $(00l)$ reflections are observed for the single crystal, suggesting that the plate-like single crystal is grown along c -axis. The full width of half maximum (FWHM) in the rocking curve of the (006) reflection is 0.12° , suggesting the high quality of the single crystal. Elemental analysis obtained by Energy Dispersive X-ray Spectroscopy (EDX) gives the atomic ratio of La : O : Mn : Se is roughly 24.21 : 33.98 : 22.02 : 19.79, suggesting the single crystal has a little Se vacancies due to high temperature melt growing. Figure 4b shows the temperature dependence of resistivity ρ_{ab} for the single crystal sample. It also show semicon-

ducting behavior as same as polycrystalline sample. The room temperature resistivity of single crystal ($\rho_{ab}=10^2 \Omega \text{ cm}$) is three orders of magnitude smaller than that of polycrystalline sample. The obtained activation energy E_a is 80.6 meV. There are several factors that lead to a huge difference of resistivity between single crystal and polycrystal. Firstly, there are a little Se vacancies in the single crystal sample, which will lead some carriers into system and increase its conductivity. Secondly, the resistance of polycrystalline sample is an average of out-plane and in-plane resistance. However, the in-plane conductance should be larger than that of out-plane since these compounds have a two-dimensional layered structure. In addition, it is more difficult to obtain an accurate resistivity for polycrystalline sample due to the impact of grain boundary effect and loose density of pressed powder sample. The susceptibility of the single crystal is shown at Fig. 4c. The high-temperature $\chi(T)$ shows a broad maximum around 350 K when magnetic field is applied in ab -plane, which is a little lower than that observed in the polycrystalline sample, and monotonically decreases as the field is applied along c -axis. With further decreasing temperature, a pronounced downward kink is observed at 161 K in $\chi(T)$ when field is applied along c -axis, indicating an AFM transition with $T_N = 161$ K. However, an obvious increase appears below this temperature in $\chi(T)$ as field applied within ab -plane. This anisotropic behavior can be understood within a scenario of a canted AFM ordering, that is, the spins ordered along c -axis antiferromagnetically, while canted in the ab -plane. Therefore, the in-plane component of spins is aligned ferromagnetically with the magnetic field applied within ab -plane. Several magnetic structure models (AFM1 or AFM6 with spin align c -axis) have been suggested in the Fe analogue and Co analogue by first principle calculation[23–26]. However, Free et al.[30] suggested AFM3-type with majority spin direction in ab plane magnetic structure in $(\text{LaO})_2\text{Fe}_2\text{Se}_2\text{O}$, similar to that in FeTe [31]. To completely understand the magnetic structure, people need detailed neutron scattering experiment to confirm for Mn analogues.

In order to further confirm the magnetic transition, the heat capacity is measured between 2 K and 400 K by a relaxation-time method in PPMS. There is a very slight anomaly around 161 K for $(\text{LaO})_2\text{Mn}_2\text{Se}_2\text{O}$ and 101 K for $(\text{BaF})_2\text{Mn}_2\text{Se}_2\text{O}$ in specific heat measurement, respectively, shown in Fig. 5, being consistent with the susceptibility anomaly. To easily distinguish specific heat anomaly, the C_p/T vs. T curves are plotted in the inset of Fig.5. These magnetic and calorimetric anomalies suggest the existence of a three dimensional long range order AFM transition evolved from high temperature low dimensional AFM or short range ordering. Comparing with Mn analogues, the Fe analogues and Co analogues had a sharp peak in specific heat around T_N . It suggests that there is more strong frustrated magnetic correlation in Mn analogues than Fe or Co analogues above T_N . It maybe leads to a low dimension AFM order in Mn ana-

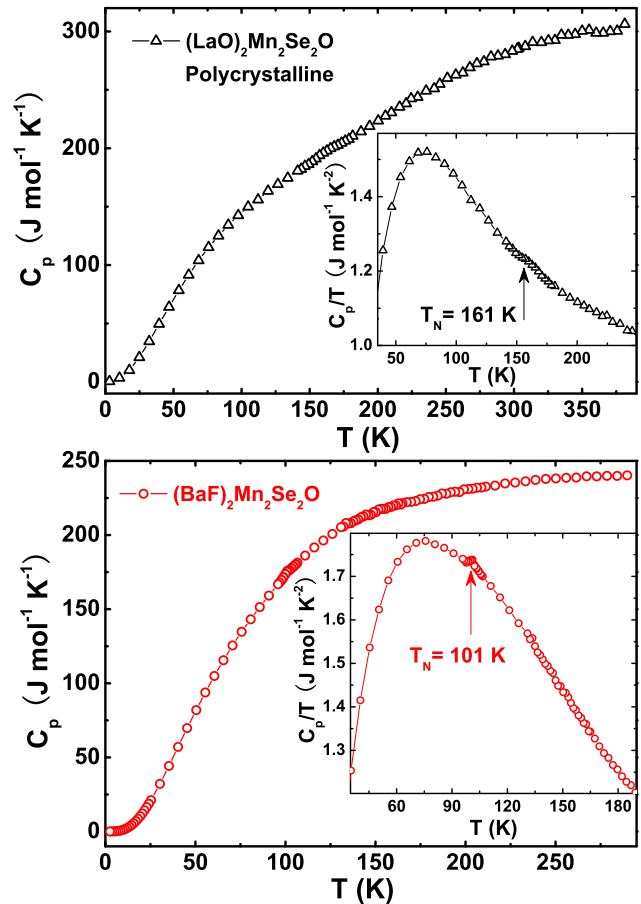


FIG. 5: Temperature dependence of specific heat for polycrystalline $(\text{LaO})_2\text{Mn}_2\text{Se}_2\text{O}$ (top panel) and $(\text{BaF})_2\text{Mn}_2\text{Se}_2\text{O}$ (bottom panel). There are weak anomaly around 161 K for $(\text{LaO})_2\text{Mn}_2\text{Se}_2\text{O}$ and 101 K for $(\text{BaF})_2\text{Mn}_2\text{Se}_2\text{O}$ in C_p/T vs. T curves, shown in the insets of top and bottom panel, respectively.

logues above T_N so that only a partial magnetic entropy is lost below the anomalous temperature.

IV. CONCLUSION

The new layered manganese oxychalcogenides $(\text{LaO})_2\text{Mn}_2\text{Se}_2\text{O}$ and $(\text{BaF})_2\text{Mn}_2\text{Se}_2\text{O}$ were successfully synthesized. Their crystal structures were refined by using the model isostructural to $(\text{LaO})_2\text{Fe}_2\text{Se}_2\text{O}$. We also grew the single crystals of the former compound using high temperature flux method. The susceptibility of as-grown single crystal samples have strong anisotropic magnetic properties below T_N , and the spins spontaneously align predominantly along the c -axis. While being an analogue to the isostructural iron and cobalt oxychalcogenides, Mn-based compounds maybe also belong to a Mott insulator with an antiferromagnetic ground state. A broad maximum of the susceptibility

observed above T_N suggests that these two-dimensional checkerboard spin lattice with a considerably strong magnetic frustration maybe form a short-range magnetic ordering or low-dimensional AFM ordering above T_N . These intrinsic magnetic behaviors are helpful in understanding the underlying physics of these rare transition metal oxychalcogenides or oxypnictides with a frustrated AFM checkerboard spin lattice.

V. ACKNOWLEDGMENT

This work is supported by the National Natural Science Foundation of China(973 Program No:2011CB00101

and Grant No. 51021091), the Ministry of Science and Technology of China, and Chinese Academy of Sciences.

Notes: As we are preparing the manuscript, we note that the compound $(\text{LaO})_2\text{Mn}_2\text{Se}_2\text{O}$ has been synthesized by Ni *et al.* and a G-type AFM order has been suggested by neutron scattering experiment at low temperature, in accepted articles list of Physical Review B.

-
- [1] J. G. Bednorz, K. A. Z. Müller, Phys. B: Condens. Matter, **64**, 189 (1986).
- [2] R. J. Cava, H. Tahgi, H. W. Zandbergen, J. J. Krajewski, Jr., W. F. Peck, T. Siegrist, B. Batlogg, R. B. van Dover, R. J. Felder, K. Mizuhashi, J. O. Lee, H. Eisaki, S. Uchida, Nature **367**, 252 (1994).
- [3] Y. Maeno, H. Hashimoto, K. Yoshida, S. Nishizaki, T. Fujita, J. G. Bednorz and F. Lichtenberg, Nature **372**, 532 (1994).
- [4] K. Takada, H. Sakurai, E. Takayama-Muromachi, R. A. Dilanian, T. Sasaki, Nature **422**, 53 (2003).
- [5] R. von Helmolt, J. Wecker, B. Holzapfel, L. Schultz, K. Samwer, Phys. Rev. Lett. **71**, 2331 (1993).
- [6] T. Kimura, Y. Annu. Tokura, Rev. Mater. Sci. **30**, 451 (2000).
- [7] P. W. Anderson, Science **235**, 1196 (1987).
- [8] Y. Kamihara, T. Watanabe, M. Hirano, and H. Hosono, J. Am. Chem. Soc. **130**, 3296 (2008).
- [9] X. H. Chen, T. Wu, G. Wu, R. H. Liu, H. Chen, D. F. Fang, Nature **354**, 761 (2008).
- [10] C. Cruz, Q. Huang, J. W. Lynn, J. Li, W. Ratcliff, J. L. Zarestky, H. A. Mook, G. F. Chen, J. L. Luo, N. L. Wang, et al., Nature **453**, 899 (2008).
- [11] Jun. Zhao, D. T. Adroja, Dao-Xin. Yao, R. Bewley, Shiliang. Li, X. F. Wang, G. Wu, X. H. Chen, Jiangping. Hu, Pengcheng. Dai, Nature Physics **5**, 555 (2009).
- [12] Q. Si, E. Abrahams, Phys. Rev. Lett. **101**, 076401 (2008).
- [13] Masatoshi Imada; Atsushi Fujimori; Yoshinori Tokura. Rev. Mod. Phys. **70**, 1039 (1998).
- [14] A. Adam,; H.-U. Z. Schuster, Z. Anorg. Allg. Chem., **584**, 150 (1990).
- [15] J. M. Mayer, L. F. Schneemeyer, T. Siegrist, J. V. Waszczak, B. V. Dover, Angew. Chem., Int. Ed. Engl. **31**, 1645 (1992).
- [16] E. A. Axtell, ; III, Tadashi Ozawa, Susan M. Kauzlarich, Rajiv R. P. Singh, Journal of Solid State Chemistry **134**, 423 (1997).
- [17] W. E. Pickett, Phys. Rev. B **58**, 4335 (1998).
- [18] Tadashi C. Ozawa, Rigo. Pantoja, Enos A. Axtell, III, Susan M. Kauzlarich, John E. Greedan, Mario. Bieringer, James W. Richardson Jr, Journal of Solid State Chemistry **153**, 275-281 (2000).
- [19] Tadashi C. Ozawa, Susan M. Kauzlarich, Mario. Bieringer, John E. Greedan, Chem. Mater. **13**, 1804 (2001).
- [20] Tadashi C. Ozawa, Susan M. Kauzlarich, Journal of Crystal Growth **265**, 571 (2004).
- [21] R. H. Liu, D. Tan, Y. A. Song, Q. J. Li, Y. J. Yan, J. J. Ying, Y. L. Xie, X. F. Wang and X. H. Chen, Phys. Rev. B **80**, 144516 (2009).
- [22] R. H. Liu, Y. A. Song, Q. J. Li, J. J. Ying, Y. J. Yan, Y. He, X. H. Chen, Chem. Mater., **22**, 1503 (2010).
- [23] H. Kabbour, E. Janod, B. Corraze, M. Danot, C. Lee, M. H. Whangbo, L. Cario, J. Am. Chem. Soc. **130**, 8261 (2008).
- [24] Jian-Xin. Zhu, Rong. Yu, Hangdong. Wang, Liang L. Zhao, M. D. Jones, Jianhui. Dai, Elihu. Abrahams, E. Morosan, Minghu. Fang, Qimiao. Si, Phys. Rev. Lett. **104**, 216405 (2010).
- [25] C. Wang, M. Q. Tan, C. M. Feng, Z. F. Ma, S. Jiang, Z. A. Xu, G. H. Cao, K. Matsubayashi, Y. Uwatoko, J. Am. Chem. Soc. **132**, 7069 (2010).
- [26] H. Wu, Phys. Rev. B **82**, 020410(R)(2010).
- [27] J. B. Goodenough, Phys. Rev **100**, 564 (1955).
- [28] D. G. Wickham and J. B. Goodenough, Phys. Rev **115**, 1156 (1959).
- [29] C. G. Shull, W. A. Strauser, and E. O. Wollan, Phys. Rev **83**, 333 (1951).
- [30] David G. Free and John S. O. Evans, Phys. Rev. B **81**, 214433 (2010).
- [31] Wei Bao, Y. Qiu, Q. Huang, M. A. Green, P. Zajdel, M. R. Fitzsimmons, M. Zhernenkov, S. Chang, Minghu Fang, B. Qian, E. K. Vehstedt, Jinhu Yang, H. M. Pham, L. Spinu, and Z. Q. Mao, Phys. Rev. Lett. **102**, 247001 (2009).